Neuro-Oncology
23(2), 240–250, 2021 | doi:10.1093/neuonc/noaa247 | Advance Access date 1 November 2020

DNA methylation based glioblastoma subclassification is related to tumoral T-cell infiltration and patient survival

Joost Dejaegher, Lien Solie, Zoé Hunin, Raf Sciot, David Capper, Christin Siewert, Sofie Van Cauter, Guido Wilms, Johan van Loon, Nadine Ectors, Steffen Fieuws, Stefan M. Pfister, Stefaan W. Van Gool, and Steven De Vleeschouwer

Research Group Experimental Neurosurgery and Neuroanatomy, KU Leuven, Leuven, Belgium and Leuven Brain Institute (J.D., L.S., Z.H., J.V.L., S.D.V.); Department of Pathology, University Hospitals Leuven, Leuven, Belgium (R.S.); Charité–Universitätsmedizin Berlin, corporate member of Freie Universität Berlin, Humboldt-Universität zu Berlin; Berlin Institute of Health, Department of Neuropathology, Berlin, Germany; and German Cancer Consortium (DKTK), Partner Site Berlin, German Cancer Research Center (DKFZ), Heidelberg, Germany (D.C.); Department of Radiology, University Hospitals Leuven, Leuven, Belgium (G.W., S.V.C.); Department of Medical Imaging, Ziekenhuis Oost Limburg, Genk, Belgium (S.V.C.); Biobank, University Hospitals Leuven, Leuven, Belgium (N.E.); Interuniversity Center for Biostatistics and Statistical Bioinformatics, KU Leuven, University of Leuven and University of Hasselt, Leuven, Belgium (S.F.); Hopp Children's Cancer Center Heidelberg, German Cancer Research Center and German Cancer Consortium, and University Hospital Heidelberg, Heidelberg, Germany (S.M.P.); Immun-Onkologisches Zentrum Köln, Köln, Germany (S.W.V.G.); German Cancer Consortium, Partner Site Berlin, German Cancer Research Center, Heidelberg, Germany (C.S.)

Corresponding Author: Joost Dejaegher, University Hospitals Leuven, Department of Neurosurgery, Herestraat 49, 3000 Leuven, Belgium (Joost.dejaegher@uzleuven.be).

Abstract

Background. Histologically classified glioblastomas (GBM) can have different clinical behavior and response to therapy, for which molecular subclassifications have been proposed. We evaluated the relationship of epigenetic GBM subgroups with immune cell infiltrations, systemic immune changes during radiochemotherapy, and clinical outcome.

Methods. 450K genome-wide DNA methylation was assessed on tumor tissue from 93 patients with newly diagnosed GBM, treated with standard radiochemotherapy and experimental immunotherapy. Tumor infiltration of T cells, myeloid cells, and Programmed cell death protein 1 (PD-1) expression were evaluated. Circulating immune cell populations and selected cytokines were assessed on blood samples taken before and after radiochemotherapy.

Results. Forty-two tumors had a mesenchymal, 27 a receptor tyrosine kinase (RTK) II, 17 RTK I, and 7 an isocitrate dehydrogenase (IDH) DNA methylation pattern. Mesenchymal tumors had the highest amount of tumor-infiltrating CD3+ and CD8+ T cells and IDH tumors the lowest. There were no significant differences for CD68+ cells, FoxP3+ cells, and PD-1 expression between groups. Systemically, there was a relative increase of CD8+ T cells and CD8+ PD-1 expression and a relative decrease of CD4+ T cells after radiochemotherapy in all subgroups except IDH tumors. Overall survival was the longest in the IDH group (median 36 mo), intermediate in RTK II tumors (27 mo), and significantly lower in mesenchymal and RTK I groups (15.5 and 16 mo, respectively).

Conclusions. Methylation based stratification of GBM is related to T-cell infiltration and survival, with IDH and mesenchymal tumors representing both ends of a spectrum. DNA methylation profiles could be useful in stratifying patients for immunotherapy trials.

Key Points

1. DNA methylation-based subclasses of GBM are related to local T cell infiltration
2. IDH and mesenchymal are immunologically distinct methylation classes

Importance of the Study

Despite the immense laboratory and preclinical research in the field of gliomas, clinical progress for patients suffering from glioblastoma has been very limited. One of the factors leading to failure of promising new treatments is most likely the heterogeneity of glioblastoma itself. We aimed to map the immunological landscape for different glioblastoma methylation subclasses, both in the microenvironment as well as in the circulating immune cells. We show that certain methylation patterns of tumor cells are related to infiltration of T lymphocytes in the tumor tissue. Furthermore, we found evidence that these methylation patterns are related to intriguing shifts in immune cells in the blood during therapy. We believe that our study adds important knowledge to our understanding of glioblastomas, and demonstrates the importance of stratifying tumor samples in the context of immunotherapy trials.

Glioblastoma (GBM) is the most frequent adult primary intrinsic brain tumor.[1] Current standard treatment consists of maximal safe neurosurgical resection followed by radiotherapy and temozolomide (TMZ) chemotherapy but only stabilizes the disease temporarily. Most patients develop a recurrence within the first year after diagnosis, and median survival is only 15 months.[2] Recently, different immunotherapeutic strategies have been explored as a potential fourth treatment modality,[3] but thus far no randomized clinical trials have been able to show a clear survival benefit. Histopathologically similar GBM can mask a heterogeneous group of tumors that probably respond differently to specific treatments. To account for this heterogeneity, several biological subclassification systems have been developed. The best known subclassification is based on the presence of a mutation in isocitrate dehydrogenase (IDH)1 or 2.[4] The majority (95%) of adult GBM do not harbor IDH mutations. IDH mutation status has recently been integrated in the standard classification of all diffuse gliomas, including GBM.[5] In research, more extensive subgroups of GBM based on genome-wide gene expression patterns have been described,[6] thus far without any real translation to the clinical arena. In 2006 Phillips et al identified 3 prognostic subgroups in a dataset of malignant grade III and IV gliomas, named proneural, proliferative, and mesenchymal.[7] The proneural class contained nearly all grade III lesions, but IDH mutation status was not included in this classification. In 2010 Verhaak et al described 4 subgroups: classical, neural, proneural, and mesenchymal. These subgroups were correlated with specific mutations and DNA copy number variations.[8] Mutations of IDH1 were almost exclusively seen in the proneural group and mutations of epidermal growth factor receptor (EGFR) were typical for the classical group. Another classification method is based on the assessment of promoter-associated hypermethylation of specific gene loci.[6] These epigenetic changes can affect gene expression and cellular function. The presence of O^6-methylguanine-DNA methyltransferase (MGMT) promoter methylation is predictive for increased benefit from TMZ chemotherapy[9] and used routinely in clinical practice. In 2012, Sturm et al published a comprehensive subclassification in 6 GBM groups based on characteristic DNA methylation patterns[10]: K27, G34, IDH1, RTK I, RTK II, and mesenchymal. K27 and G34 are mainly pediatric or adolescent GBM. These subgroups were correlated with certain chromosomal aberrations, mutations, or gene amplifications. The RTK I group is enriched for platelet-derived growth factor receptor A amplification (PDGFRA). The RTK II group is characterized by chromosome 7 gain, chromosome 10 loss, cyclin-dependent kinase inhibitor 2A CDKN2A loss and amplification of epidermal growth factor receptor (EGFR). The IDH group has global DNA hypermethylation. The mesenchymal group has no typical point mutations and showed a lower incidence of typical GBM genetic alterations. Although overlap was seen with the Verhaak classification, DNA methylation profiling does not exactly match with gene expression based subclasses.[11] Recently, this DNA methylation-based classification has been expanded for use in almost all known central nervous system tumors.[12]

In our research group at KU Leuven, a translational research program investigating postoperative administration of dendritic cells (DCs) loaded with autologous tumor lysate to induce antitumor immunity has been carried out for more than a decade.[13,14] In the presented "GliomaTranslat" study, we stratified tumor tissue of newly diagnosed GBM patients treated with postoperative radiochemotherapy and early or late DC vaccination, according to the DNA methylation based classification developed by Sturm et al.[10] Subsequently, we correlated these subgroups with infiltrating immune cells, changes in systemic immune cells and survival.

Material and Methods

Patients, Clinical Data, and Tumor Tissue

Clinical data, tumor tissue, and blood samples were prospectively collected from 132 patients with newly diagnosed primary GBM. All patients underwent a total or subtotal resection between 2010 and 2014 and had a postoperative Karnofsky performance index of at least 70. After confirmation of pathology, patients were proposed a treatment with adjuvant experimental DC vaccination. After written informed consent, patients were treated with standard radiochemotherapy and DC vaccination. Progression was determined on serial MRI scans by a reference radiologist (G.W.). Overall survival (OS) was determined as the interval between surgical resection of the primary lesion and death. Extent of resection (EOR) was scored on an early postoperative MRI scan (<72 hours after surgery) as total, subtotal or partial (respectively no,

<2 cm^3 and >2 cm^3 contrast enhancing tissue). In 9 patients this early MRI was not available, and EOR was determined based on the intraoperative assessment of the neurosurgeon and first available postoperative CT and/or MRI scan.

This initial consent contained the possibility to give explicit consent for (or specific objection against) the use of leftover samples for scientific research after the immunotherapy was ended. None of the patients objected. 13 patients who did not give explicit consent and were still alive at the start of the GliomaTranslat study were contacted and received a new informed consent, of whom 11 approved. Two patients did not sign the additional informed consent. Leftover tissue and blood samples of patients who were deceased at the start of the Glioma Translat study could be used for scientific research according to Belgian law and after positive advice of the local ethical committee. Of the 130 included patients, 105 had leftover formalin-fixed and paraffin-embedded (FFPE) tumor tissue available for analysis. These samples were reviewed by the reference pathologist (R.S.) to select parts with high content of viable tumor tissue. A schematic overview of the inclusion process is given in Supplementary Figure 1.

Methylation Data Analysis and Classification Methodology

Genome-wide DNA methylation was performed as described by Sturm et al.[10] For this, 20 unstained sections of 5 µm were prepared from the representative FFPE blocks, as well as reference flanking hematoxylin and eosin (HE) sections. Methylation data were generated using the HumanMethylation 450 Bead Chip (Illumina). For comparison, data of this study were analyzed together with methylation data of CNS tumors and normal tissue.[12] Raw intensity signals were read and normalized with minfi version 1.32.0 and DNA Array version 2.1 in parallel with the BiocParallel version 1.20.1. Probes with a *P*-value >0.01 in more than 10% of the samples are filtered out, as well as probes located on sex chromosomes, containing a single-nucleotide polymorphism, or probes which were cross-reactive and polymorphic in the microarray chip.[15] Beta values were calculated, filtered, and sorted for the 25000 most variable methylated probes. A *t*-distributed stochastic neighbor embedding analysis (t-SNE), comprising the samples generated for this study together with all samples from the study of Capper et al,[12] was performed with the Rtsne package version 0.15 with the following parameters: theta = 0.5, pca = TRUE, perplexity = 30 and max_iter = 5000. Hierarchical clustering was performed with the agglomeration method "ward.D2." The distance was calculated with the Euclidean method for clustering and sorting the samples with packages factoextra version 1.0.7 and dendsort version 0.3.3. Again, the most 25000 cytosine-phosphate-guanines (CpGs) were used for calculation. The heat map was visualized with the heatmap package version 1.0.012.

Samples were then classified using the experimental version v12.0 of the MolecularNeuropathology.org brain tumor classifier, with a molecular family cutoff of 0.84[16] and a molecular class cutoff of 0.5.[12] In 6 of these 105 samples, methylation analysis could not identify tumor tissue, and 3 samples were reclassified after DNA methylation analysis (2 as oligodendroglioma and 1 as ependymoma). Of the remaining 96 samples, 65 samples were directly classified into a methylation group. The t-SNE analysis with the entire reference cohort was then used to elucidate the nature of the other 31 cases (Supplementary Figure 2). Here we found that all these cases except 3 grouped together with the glioblastoma IDH wildtype family, and did not form a separate group. The 3 outlier cases were grouped close to normal brain samples of the reference cohort and indeed had a low tumor cell content on histology, albeit still representing GBM. These samples were excluded from further analysis. For the other 28 unclassifiable samples, we performed an unsupervised clustering to classify them into 19 mesenchymal, 8 RTK I, and 1 RTK II (Supplementary Figure 3). For MGMT promoter methylation, the cutoff score of 0.358 was used according to Bady et al.[17]

Immunohistochemistry

Five-micrometer sections were prepared and stained for cluster of differentiation (CD)3, CD8, forkhead box (Fox)P3, CD68, and PD-1. A detailed list of the primary antibodies and staining methods is given in Supplementary Methods. Infiltrative (not perivascular) CD3+ T and CD8+ cells were assessed quantitatively. The whole sample was reviewed at low resolution (4x). In parts of viable nonnecrotic tumor tissue, 10 high power fields (HPF; 400x magnification; 40x objective × 10x ocular)) were randomly selected, and infiltrating CD3+ T cells were counted. The sum of 10 HPF was used as total CD3+ count. The same strategy was used for CD8+ T cells. FoxP3+ density was assessed qualitatively as "absent," "present," or "abundant." For PD-1 expression, a hot spot approach was used as described by other research groups[18]: Areas with obvious CD3+ infiltration were identified and scored "PD-1 positive" as >1 PD-1 positive cell and "abundant" as >5 PD-1 positive cells per HPF were seen, respectively. Infiltrative CD68+ cells were assessed qualitatively as present in <25%, 25–50%, and >50% of tumor tissue. Examples of the different histology scores are given in Figure 1A–F.

Immune Cell Isolation and Flow Cytometry

A first blood sample was drawn 1–2 weeks after surgery, after withdrawal of steroids, but before the start of concomitant radiochemotherapy (referred to as *before RC*). A second sample was taken after concomitant radiochemotherapy but before the start of adjuvant temozolomide (*after RC*). MRI scans were organized every 3 months or earlier upon clinical progression. Peripheral blood mononuclear cells (PBMCs) were isolated from fresh blood samples by centrifugation in a density gradient (Lymphoprep, Fresenius Kabi) as previously described.[19] Purified PBMCs were dissolved in human serum albumin (HSA; Baxter) with 10% DMSO (CryoSure-DMSO, WAK-Chemie) and stored in liquid nitrogen until use. For flow cytometry, all samples of a single patient were thawed, stained, and analyzed together as described before.[19] Detailed antibody panels and staining protocol are given in Supplementary Methods.

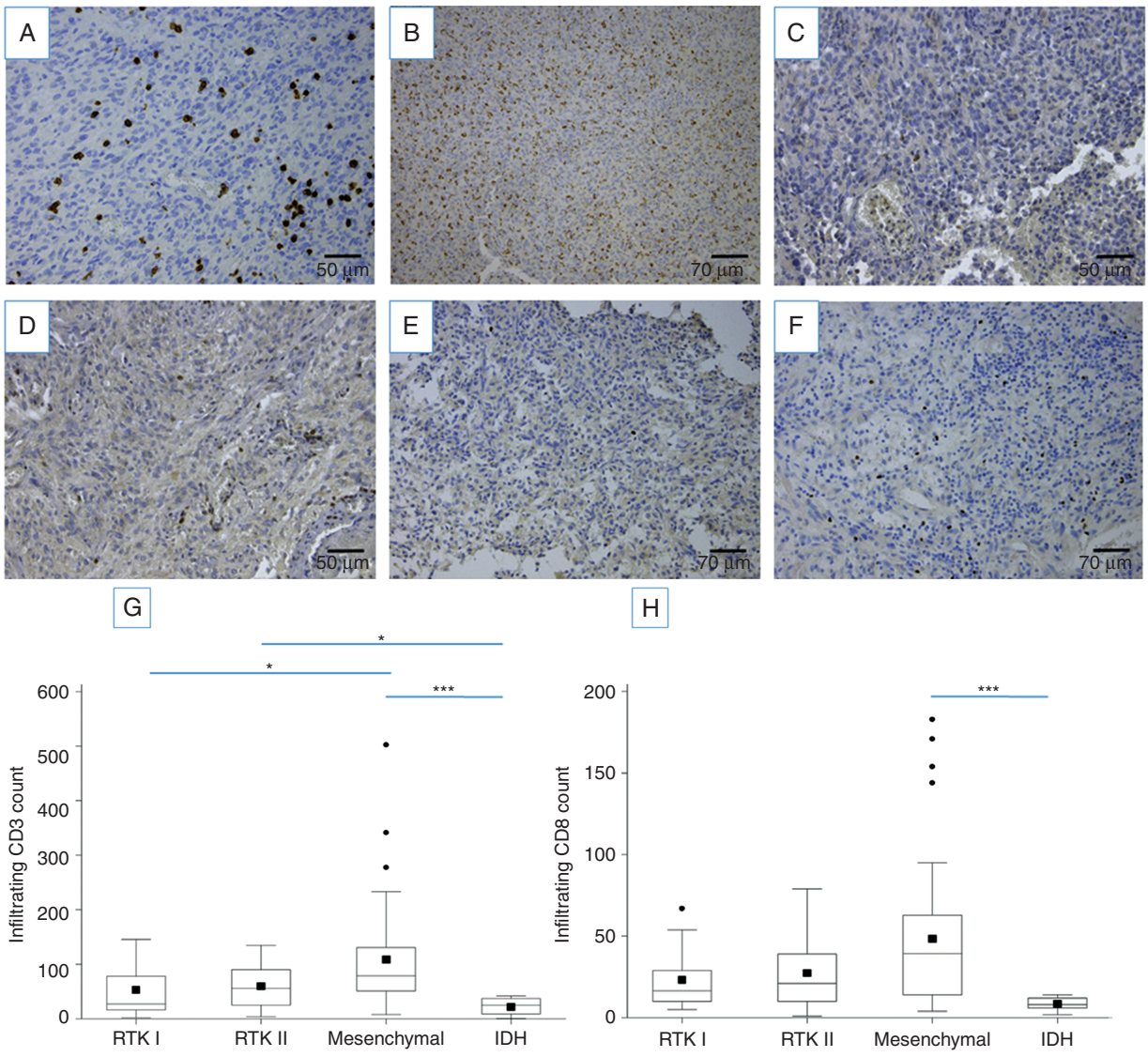

Fig. 1 Infiltrating CD3+ and CD8+ cells were counted in 10 randomly chosen HPFs (A). CD68+ infiltration was scored as present in >25, 25–50 or >50% of the whole tumor sample (B). PD-1 was evaluated using a hotspot approach, and scored positive if >1 cell per HPF (C) or obvious (D) if >5 cells per HPF were seen. FoxP3 infiltration was scored as absent, present (E) or abundant (F). The total number of counted CD3+ cells (G) and CD8+ cells (H) for each methylation class is given. Significant differences in pairwise comparisons are indicated (*$P < 0.05$, ***$P < 0.005$).

Cytokine Analysis

Fresh blood samples were allowed to clot for at least 15 minutes and were then centrifuged to obtain serum. Fresh serum was stored at –80 °C until use. All serum samples of a single patient were thawed and analyzed together. A set of cytokines was selected based on literature and previous experience in the lab: interleukin (IL)-10, IL-12, Vascular endothelial growth factor (VEGF), interferon gamma (IFN-ɣ), monocyte chemoattractant protein 1 (MCP-1), and galectin (Gal)-1. For galectin-1, ELISA (enzyme-linked immunosorbent assay) with a goat anti-human galectin-1 antibody was used as described.[20] For the other cytokines, cytometric bead assay (CBA) was performed following the manufacturer's protocol (Becton Dickinson [BD]). Acquisition was done with the BD SR Fortessa 2 and analysis with FCAP Array Software.

Statistical Analysis

Univariable Cox proportional hazards regressions models were used to test for the association between methylation subgroups and the immunohistochemistry data on the one hand and survival time on the other hand. Survival time was determined as the time between date of surgical resection and death. Patients alive were censored. To control for established prognostic variables as age, EOR, MGMT

promoter status, and the treatment variable of early versus late vaccination, a multivariable Cox model was constructed controlling for these factors. Survival curves were constructed using Kaplan–Meier estimates.

Immunohistochemistry data were compared between the methylation classes using 1-way ANOVA. To obtain a more symmetric distribution of the model residuals, the analysis was performed on log-transformed values when needed. Bonferroni or Tukey corrected *P*-values were reported for the pairwise comparisons if the overall test was significant.

Blood immune parameters were analyzed with a linear mixed model for repeated measures to compare the evolution over the 2 time moments (before and after RC). This model can handle missingness in the longitudinally measured data and contained a random subject intercept to handle the correlation between the measurements before and after RC. The model contained main effects of time and methylation subclassification. The interaction term was added to verify if the evolution over the 2 moments differed between the methylation subclassifications. Least-squares means (and 95% confidence intervals) from these models were reported. If the interaction was significant, pairwise comparisons of the changes were performed, applying a Bonferroni correction for multiple testing.

For the analysis of OS as function of infiltration T-cell counts and blood immune values, results were obtained from a Cox regression, allowing nonlinearity (on the log hazard scale) using restricted cubic splines.

An alpha level of 0.05 was considered as significant in all analyses. Reported *P*-values were two-sided. Given the large number of performed tests, a single significant *P*-values needs to be interpreted with caution. All analyses have been performed using R version 3.3.3 (2017-03-06) in Rstudio. The mixed-effect model was performed by the nlme package (https://cran.r-project.org/web/packages/nlme/index.html).

Results

A detailed case by case list of all 93 samples is given in Supplementary Table 1. This gives case-by-case details including information on clinical data, methylation class prediction, and interpretation of classification. Furthermore, immunohistochemistry and flow cytometry results are given.

Patient Methylation Profile Characteristics

Of the 93 tumor samples, 42 had a mesenchymal, 27 an RTK II, 17 a RTK I, and 7 an IDH DNA methylation pattern (Table 1). Patients in the IDH subgroup were younger than patients in other subgroups, although this was not statistically significant. There were no significant differences in sex, EOR, and early or late vaccination.

Table 1. Patient characteristics, PFS and OS in different DNA-methylation based subgroups of GBM. PFS and OS are given in months after first surgery. *P*-values for OS and PFS in this table were determined in multivariate analyses

	Mesenchymal	RTK II	RTK I	IDH	*P*-value
Number of patients	42	27	17	7	
Age					
Median	61	60	60	46	**0.069**
Mean	58.6	58.9	58.7	48	
Range	38–70	44–70	44–70	36–64	
Sex					
male / female	31 / 11	13 / 14	12 / 5	5 / 2	**0.174**
% male	*73.8*	*48.2*	*70.6*	*71.4*	
Extent of resection					
Partial	4	1	5	2	**0.13**
Subtotal	16	8	5	3	
Total	22	18	7	2	
% Total	*52.4*	*66.7*	*41.2*	*28.6*	
DC Vaccination					
Early / late	21 / 21	15 / 12	7 / 10	4 / 3	**0.82**
% early	*50*	*55.6*	*41.8*	*57.1*	
Median PFS	3	11	10	24	**0.0078**
Median OS	15.5	24	16	36	**0.0074**

Infiltrating Immune Cells According to DNA Methylation Profile

A detailed overview of all immunohistochemistry data is given in Supplementary Table 1. Immunohistochemistry for assessment of CD3+ T cells and PD-1 expression was available in 89 samples, and for CD8+, FoxP3+, and CD68+ myeloid cells in 91 samples. Mesenchymal tumors had the highest amount of infiltrating CD3+ T cells and IDH tumors the lowest (median 79 vs 25 CD3+ T cells in 10 HPFs, respectively) (Figure 1G, Supplementary Table 2). The difference between tumor groups was highly significant ($P = 0.0001$). In a pairwise comparison between different methylation classes, significantly higher CD3+ counts in mesenchymal tumors than IDH and RTK I tumors were found (Supplementary Table 3A).

As for the CD3+ T cells, we found the highest counts of CD8+ T cells in mesenchymal tumors and the lowest in IDH tumors (median 39.5 vs 8 per 10 HPF, respectively, overall $P = 0.0017$). In a pairwise comparison, the difference between mesenchymal and IDH tumors was significant (Figure 1H, Supplementary Table 3B). There was a clear correlation between CD3+ and CD8+ counts, although in 14 samples a higher CD8+ than CD3+ count was found (Supplementary Figure 4).

PD-1+ cells were assessed qualitatively, and 39/89 (43.8%) samples showed PD-1 positivity. Differences were not significant between groups, although only 1 PD-1 positive IDH tumor was seen. FoxP3, as marker for regulatory T cells, was scored similarly. Only 1 IDH tumor was FoxP3 positive, while other subclasses showed FoxP3 expression in 25 to 46% of samples. Abundant FoxP3 positivity was only seen in 2 mesenchymal samples. Also here there was no significant difference between classes. Infiltrating CD68+ myeloid cells were scored semi-quantitatively, but no significant differences between classes were found.

Systemic Immune Changes Before and After Radiochemotherapy

Blood samples were taken before (*before RC*) and shortly after (*after RC*) concomitant radiochemotherapy, and an analysis of immune cell populations and selected cytokines was done. An example of the distribution of observed values of white blood cells and their estimates from the linear mixed model for different methylation classes is shown in Supplementary Figure 5. The statistical analysis was done for all blood parameters. Number of available samples and results are summarized in Table 2.

As expected, absolute white blood cell (WBC) count and lymphocyte counts showed a significant decrease after radiochemotherapy, but no difference between methylation classes was observed.

Irrespective of methylation class, we found in the whole group of samples shifts in T cell (sub)populations between the 2 time points. CD4+ T cells decreased relatively (median 51.8 → 41.3%), while CD8+ T cells increased (38.5 → 46.9%). The proportion of PD-1+ CD8+ cells and increased after RC (Table 2 – time effect). When differences between methylation classes were evaluated irrespective of the time point, no significant differences were found (Table 2 – meth. effect). Although there were

Table 2. Blood was drawn before (Before RC) and after (After RC) radiochemotherapy. Immune cell fractions and cytokines were determined. Median and lower and upper quartiles (Q1-Q3) are given. Statistical analysis was done using a linear mixed effect model. In this model, 3 effects were verified: (1) the effect of time on the measured values, irrespective the methylation class (time), (2) the effect of methylation class on the mean value irrespective the moment (meth. class); and (3) the interaction between time and methylation class (time * meth. class). This last effect refers to differential changes over time between methylation classes. N represents number of available samples for each analysis

	Before RC			After RC			P - value		
	N	Median	Q1-Q3	N	Median	Q1-Q3	time	meth. class	time * meth. class
WBC (x10^9/L)	93	6.3	5.2–8.4	82	5.1	4.1–6.1	**<0.001**	0.58	0.19
Lymphocytes (x10^9/L)	93	1.3	1.1–1.7	82	0.8	0.7–1.1	**<0.001**	0.34	0.14
Lymphocytes (% of WBC)	93	22.4	18.0–26.4	82	16.7	12.9–21.1	**<0.001**	0.39	0.99
CD3+ (% of total CD45+)	92	38.8	30.5–50.1	85	39.7	27.0–52.8	0.29	0.06	0.68
CD4+ (% of total CD3+)	92	51.8	39.0–61.3	85	41.3	30.3–53.6	**0.002**	0.72	**0.04**
CD8+ (% of total CD3+)	92	38.5	28.8–49.2	85	46.9	36.5–59.5	**<0.001**	0.96	**0.03**
CD4+ PD-1+ (% of total CD4+)	92	39.9	27.9–49.6	85	44.0	31.7–56.3	0.17	0.29	0.07
CD8+ PD-1+ (% of total CD8+)	92	48.4	40.1–58.1	85	63.2	50.5–71.7	**<0.001**	0.37	**0.01**
Tregs (% of total CD4+)	92	6.6	5.1–8.9	84	10.9	8.0–16.0	**<0.001**	0.53	0.87
Regulatory T cell (Treg) PD-1+ (% of total Tregs)	92	46.0	38.9–56.5	84	39.8	30.2–53.1	**0.02**	0.61	0.05
IL-10 (pg/mL)	82	3.2	1.9–4.1	83	2.5	1.6–4.0	0.16	0.26	0.30
IL-12 (pg/mL)	82	14.1	8.3–22.1	83	30.5	17.1–52.8	**<0.001**	0.65	0.53
MCP-1 (pg/mL)	82	129.7	86.7–235.1	82	126.0	87.5–175.5	**0.006**	0.79	0.47
IFN-g (pg/mL)	82	1.1	0.2–2.4	82	0.9	0.0–1.5	0.55	0.26	0.23
VEGF (pg/mL)	82	58.7	35.7–120.5	83	44.4	26.2–74.4	**0.003**	0.96	0.76
Gal-1 (pg/mL)	81	2.0	1.7–2.2	82	1.7	1.5–2.1	0.15	0.50	0.88

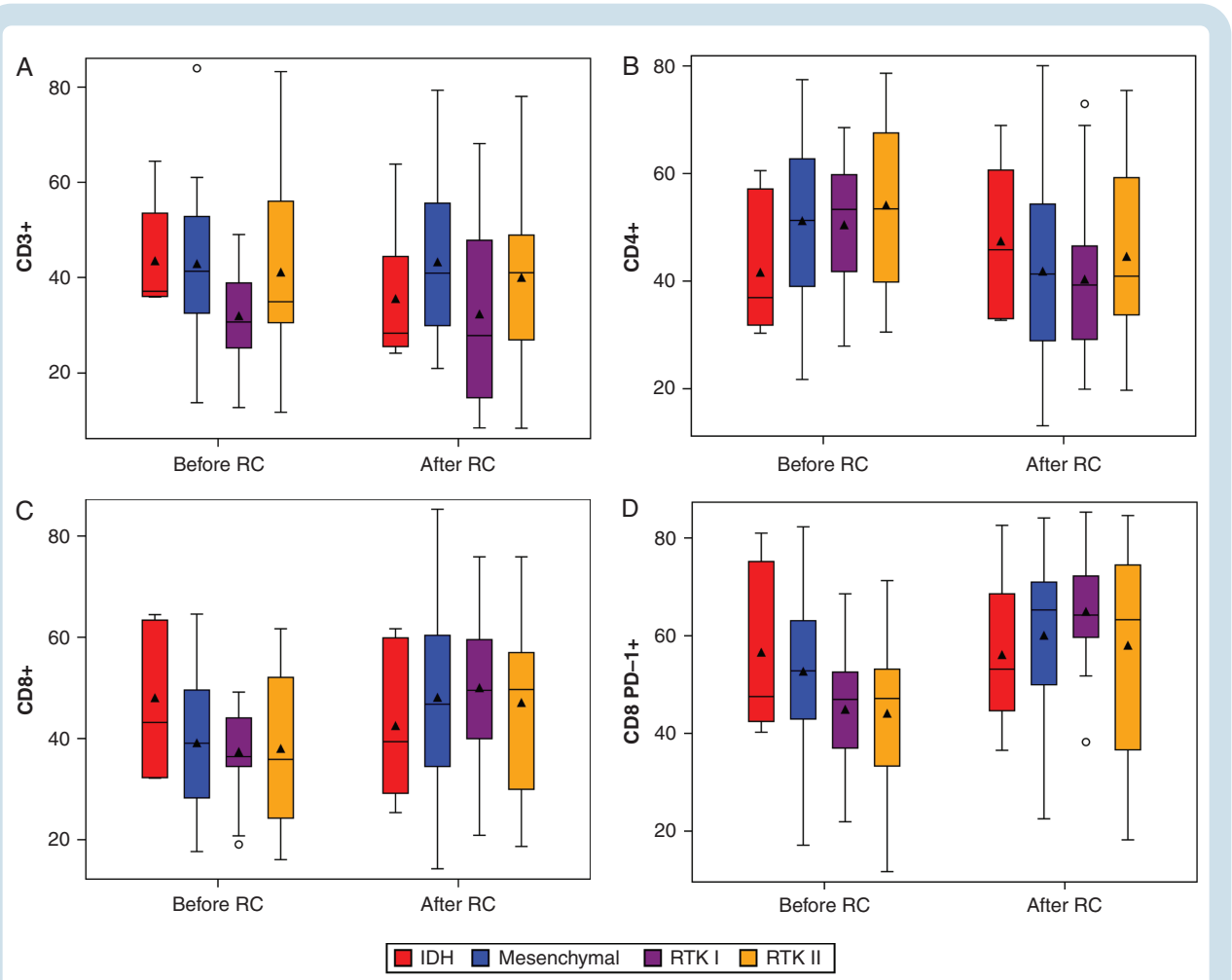

Fig. 2 Evolution of blood T-cell populations in the different methylation classes before and after radiochemotherapy. For the general CD3+ T-cell population, no significant differences were found between methylation classes (A). For CD4+ T cells (B), CD8+ T cells (C) and CD8+ PD-1+ T cells (D) subpopulations, the evolution over time was significantly different between methylation classes with *P*-values of 0.04, 0.03, and 0.01 respectively.

no differences in the evolution of the general CD3+ cell population between methylation classes (Figure 2A), significant differences are seen in T cell subpopulations. The decrease in proportion of CD4+ T cells was present in all groups, except the IDH group where we found an increase (41.6 → 47.4%, $P = 0.04$). Subsequent pairwise comparison between groups did not show significant differences. The increase in CD8+ T cells that was seen after RC was present in all groups expect the IDH group, where a relative decrease was seen (47.7 → 41.4%, $P = 0.03$). Pairwise comparison between groups showed significance between RTK I and IDH ($P = 0.025$). For PD-1 expression on CD8+ cells, we found an increase after RC for RTK I, RTK II and mesenchymal tumors, while PD-1 expression in IDH tumors remained stable (56.5 → 56.0%, $P = 0.01$) (Figure 2C, D). Pairwise comparison showed significance between RTK I and mesenchymal ($P = 0.036$) and RTK I and IDH ($P = 0.030$).

Selected cytokines were measured at the 2 time points (Table 2). After radiochemotherapy, we found a significant increase in IL-12 and significant decreases in VEGF and MCP-1. There were no changes in IL-10, IFNγ or Galectin-1. None of these changes in cytokines was related to specific methylation classes or differential evolution in time.

Survival Analysis

The amount of CD3+ T-cell infiltration was inversely correlated with OS. In univariable analysis, there was a small but significant correlation with OS with a hazard ratio (HR) of 1.035 per unit CD3 (95% CI = 1.006–1.065, $P = 0.019$). The relation is visualized allowing nonlinearity (Figure 3A). In multivariate analysis, the HR remained 1.031 but was not significant (95% CI 0.998–1.065,

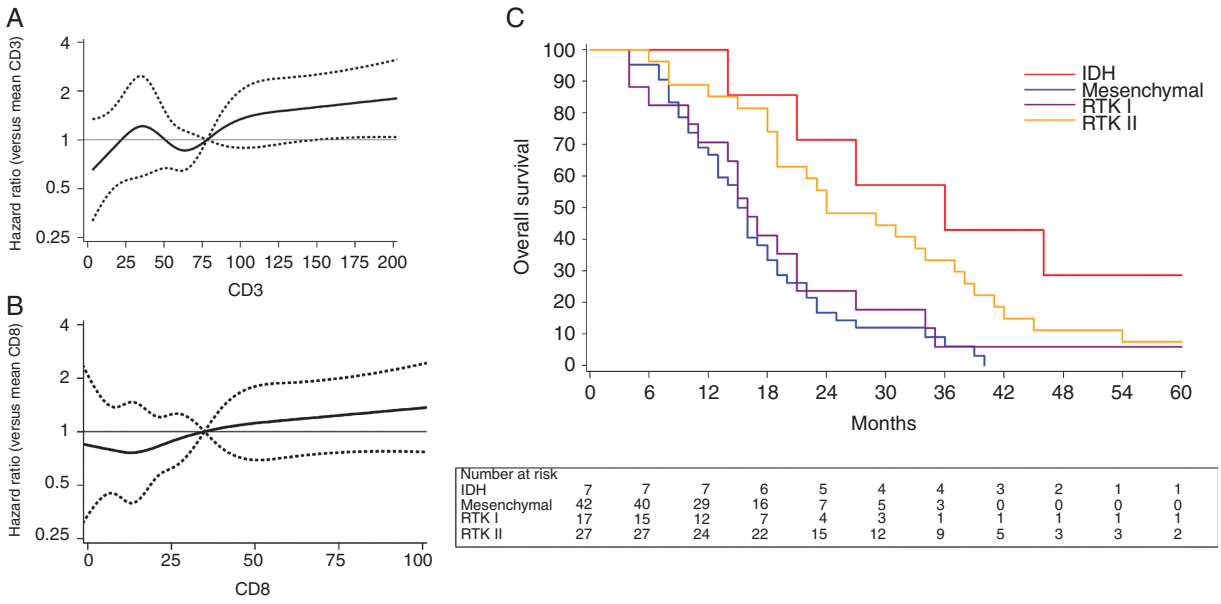

Fig. 3 Hazard ratio for death as function of infiltrating CD3+ (A) and CD8+ (B) counts, relatively to their respective mean values of 78 CD3+ and 35 CD8+ T cells. Dotted lines represent 95% confidence intervals. (C) Kaplan–Meier graph showing OS for the 4 DNA methylation subgroups of GBM patients: 36.0 months in the IDH group, 15.5 in the mesenchymal, 16.0 in the RTK I and 24.0 in RTK II group.

P = 0.065). The same trend was seen for CD8+ T-cell infiltration, without significance in univariate (HR = 1.057; CI = 0.998–1.119; P = 0.059) or multivariate analysis (HR = 1.054; CI = 0.992–1.120; P = 0.091) (Figure 3B). When looking at survival across different methylation groups, OS of tumors in the IDH group was markedly longer than those of other methylation classes (Figure 3C), and the difference was significant in univariate (P = 0.0002) and multivariate (P = 0.0074) analysis (Table 3). An extended analysis between OS and blood immune cell populations and cytokines, both before and after RC, did not show statistically significant correlations.

Discussion

In this study, we subclassified 93 glioblastomas with the DNA methylation classification developed by Sturm et al[10] to search for correlations with infiltrating and circulating immune cells. Seven patients (7.5%) had tumor samples belonging to the IDH methylation subgroup, which is characterized by global DNA hypermethylation and MGMT promoter methylation. There is a large, yet not perfect, overlap between IDH methylation groups and the presence of IDH1 mutations.[10] In the tumor microenvironment, we found these IDH tumors to have the lowest CD3+ T-cell infiltration. Using immunohistochemistry to detect IDH mutated GBM, Berghoff et al found that IDH-mutated GBM have significantly less CD3+ tumor-infiltrating cells than IDH-wildtype GBM.[21] However, while we detected CD3+ cells in all samples, Berghoff found tumor-infiltrating lymphocytes in only 21.4% of IDH-mutant and 66.7% of IDH-wildtype samples. This can be due to a different antibody and immunostaining methodology, as well as interpretation of the results. While we counted cells on a number of randomly chosen HPF, Berghoff et al used a semi-quantitative overall impression at low magnification. Anyhow, both studies suggest that IDH tumors are less infiltrated by immune cells, thereby confirming the status of immunologically "cold" tumors.

Mesenchymal tumors had the highest amount of infiltrating CD3+ T. Using gene expression based subclassification, other researchers have also documented increased lymphocytic infiltrations in mesenchymal tumors. Rutledge et al found tumor-infiltrating lymphocytes to be strongly enriched in the mesenchymal class.[22] They suggested that the mesenchymal GBM could be more immunogenic. Prins et al described an increase in CD3+ and CD8+ infiltration in tumors with the mesenchymal gene expression pattern.[23] In their phase I study investigating the use of DC vaccination in 15 newly diagnosed GBM patients, a significantly increased OS was seen in patients with mesenchymal tumors (n = 9) compared with a partially matched mesenchymal tumor control group.

The relationship between infiltrating T cells and prognosis in GBM remains controversial. In literature, positive,[24–29] absence of correlation,[22,30] or even a negative correlation[31] with OS have been reported. A table summarizing studies on T-cell infiltration in gliomas is given in Supplementary Table 4. Although not significant in multivariate analysis (P-value 0.065), we found in our patients a clear trend towards worse OS with increased infiltrating CD3+ T cells, with HR for death of 1.031 per unit increase in CD3+ T cell count. The question remains whether GBM-infiltrating lymphocytes are truly antitumoral or rather

Table 3. Univariate and multivariate analysis of Overall Survival of different DNA methylation tumor subgroups, adjusted for age at resection, EOR, early versus late vaccination and MGMT promoter methylation in a Cox proportional hazards model. # = reference category

Variable		Hazard Ratio	95% CI	*P*-value
	Univariate analysis			
Methylation subclassification				0.0002
	IDH	#	#	#
	mesenchymal	4.83	1.84 – 12.71	0.001
	RTK I	3.86	1.39 – 10.67	0.009
	RTK II	1.99	0.76 – 5.23	0.16
	Multivariate analysis			
Methylation subclassification				0.0074
	IDH	#	#	#
	mesenchymal	3.90	1.35 – 11.21	0.012
	RTK I	3.36	1.14 – 9.92	0.029
	RTK II	1.80	0.62 – 5.18	0.28
Age at resection		1.0	0.97 – 1.03	0.97
Early vs late DC vaccination				
	Early	#	#	#
	Late	0.72	0.44 – 1.15	0.17
EOR				0.42
	Partial	#	#	#
	Subtotal	0.75	0.36 – 1.58	0.45
	Total	0.62	0.30 – 1.30	0.21
MGMT promoter methylation				<0.001
	Methylated	#	#	#
	Unmethylated	2.67	1.63 – 4.37	<0.001
	Not determinable	2.0	0.76 – 5.24	0.16

anergic "bystanders," or even immunosuppressive protumoral lymphocytes.

PD-1 positive cells were detected in 44% of samples, but did not show significant association with any methylation class or OS. However, in the IDH group only 1 out of 7 samples showed weak PD-1 expression. Other methylation classes seemed to have more frequent PD-1 positive staining. In a large immunohistochemical study, Garber et al found PD-1 positive tumor-infiltrating lymphocytes (TILs) in 35% of GBM and 77.8% of gliosarcomas.[18]

To assess systemic immune cell evolutions, we used flow cytometry. By using samples taken before and after radiochemotherapy, we aimed to make this dataset as homogeneous as possible. While general WBC and lymphocyte counts decreased after radiochemotherapy, the proportion of CD3+ T cells remained stable. However, we found a shift towards increased CD8+ and decreased CD4+ cells in all methylation subgroups except IDH. Although an increase in CD8+ T cells could suggest a cytotoxic immune response, we also found these CD8+ cells to have increased expression of PD-1. We know from a previous study that, at the moment of surgery, PD-1 expression in the blood does not differ between glioma patients and healthy volunteers.[19]The current study shows that PD-1 expression in the blood increases after radiochemotherapy. This observation suggests that surviving CD8+ T cells after radiochemotherapy might evolve towards an exhausted and / or anergic phenotype.[32] Theoretically, PD-1 expression can also represent early activation, although this is less likely in the immune suppressed state after several weeks of radiochemotherapy. Intriguingly, IDH tumors did not show this evolution, but were found to have a decrease in the proportion of CD8+ T cells after radiochemotherapy with stable PD-1+ CD8+ T cells. As this was only a small group of 7 patients and differences before and after RC values were small, this finding of "systemic immune inertia" in IDH mutated GBM needs to be confirmed. Changes in systemic immunity are important during the course of GBM, but currently not fully understood. Grossman et al described that patients with CD4+ T cells <200 cells/mm^3 had a significantly decreased survival that was related to tumor progression and not to severe infections.[33] Fadul et al found a significant decrease in mean total white blood cell count and mean lymphocyte count after radiochemotherapy, without changes in the relative distribution of CD4+ and CD8+ T cells or the myeloid compartment.[34]

We did not see significant differences in CD68+ positive cells. It was shown that that mesenchymal tumors have higher numbers of tumor-associated macrophages.[35] This contrasting finding could have several reasons. Our research focused mainly on T cells and CD68+ cells were

only assessed as a general marker for myeloid cell infiltration, without further characterization. Furthermore, the qualitative (and not quantitative) assessment method and low sample size could contribute to the observed differences.

Conclusion

Immunological profiling of methylation subgroups of GBM seems to distinguish IDH tumors and mesenchymal tumors as both ends of a spectrum. Hypermethylated IDH tumors are immunologically "cold" and characterized by low amounts of tumor-infiltrating CD3+ T cells, low PD-1 expression, and a longer median OS. Mesenchymal tumors have high amounts of infiltrating CD3+T cells but a shorter median survival. Systemic immune monitoring reveals a shift toward proportionally increased PD-1 expressing CD8+ cells after radiochemotherapy, except in IDH tumors which seem more immunologically "inert." Our results strongly suggest that DNA-methylation-based stratification of GBM should be recommended in future immunotherapy trials.

Supplementary Material

Supplementary material is available online at *Neuro-Oncology* (http://neuro-oncology.oxfordjournals.org/).

Keywords

DNA methylation | glioblastoma | immune infiltration | tumor microenvironment

Funding

The research leading to the results of this project has received funding from the European Union Seventh Framework Program under grant agreement number 600841, Computational Horizons in Cancer (CHIC; www.chic-vph.eu). Other funding was received from the Olivia Fund (www.olivia.be); The Belgian Brain Tumor Support (www.bbts.be), Herman Memorial Research Foundation, and the Helaers Foundation. This research was further supported by the DKFZ-Heidelberg Center for Personalized Oncology (DKFZ-HIPO_036) program.

Acknowledgments

The authors thank Anaïs Van Hoylandt, Jonathan Creemer, and Ellen Dilissen for their technical support with flow cytometry. We thank the Microarray unit of the Genomics and Proteomics Core Facility (DKFZ) for methylation services.

Conflict of interest statement. DC and SMP have a patent pending: DNA methylation-based method for classifying tumor species (EP 16710700.2). The other authors declare no conflict of interest.

Authorship statement: Design of the Study: JD, SWVG, SDV, NE, JVL. Clinical and radiological data collection: JD, LS, ZH, SVC, GW, JVL, NE, SWVG, SDV. Pathology and molecular data collection: RS, DC, CS, SMP, SDV. Statistical analysis: SF, CS. Flow cytometry analysis: JD, LS, SDV. All authors were involved in the interpretation of data and results. Manuscript writing: JD, LS, SDV. Final editing and approval of the manuscript: JD, LS, ZH, RS, DC, CS, SVC, GW, JVL, NE, SF, SMP, SWVG, SDV. List of unpublished papers cited: none.

References

1. Ostrom QT, Gittleman H, Fulop J, et al. CBTRUS statistical report: primary brain and central nervous system tumors diagnosed in the United States in 2008–2012. *Neuro Oncol.* 2015;17(Suppl 4:iv1-iv62):1–21.
2. Stupp R, Mason WP, van den Bent MJ, et al; European Organisation for Research and Treatment of Cancer Brain Tumor and Radiotherapy Groups; National Cancer Institute of Canada Clinical Trials Group. Radiotherapy plus concomitant and adjuvant temozolomide for glioblastoma. *N Engl J Med.* 2005;352(10):987–996.
3. Fecci PE, Heimberger AB, Sampson JH. Immunotherapy for primary brain tumors: no longer a matter of privilege. *Clin Cancer Res.* 2014;20(22):5620–5629.
4. Yan H, Parsons DW, Jin G, et al. IDH1 and IDH2 mutations in gliomas. *N Engl J Med.* 2009;360(8):765–773.
5. Louis DN, Perry A, Reifenberger G, et al. The 2016 World Health Organization classification of tumors of the central nervous system: a summary. *Acta Neuropathol.* 2016;131(6):803–820.
6. Sturm D, Bender S, Jones DT, et al. Paediatric and adult glioblastoma: multiform (epi)genomic culprits emerge. *Nat Rev Cancer.* 2014;14(2):92–107.
7. Phillips HS, Kharbanda S, Chen R, et al. Molecular subclasses of high-grade glioma predict prognosis, delineate a pattern of disease progression, and resemble stages in neurogenesis. *Cancer Cell.* 2006;9(3):157–173.
8. Verhaak RG, Hoadley KA, Purdom E, et al; Cancer Genome Atlas Research Network. Integrated genomic analysis identifies clinically relevant subtypes of glioblastoma characterized by abnormalities in PDGFRA, IDH1, EGFR, and NF1. *Cancer Cell.* 2010;17(1):98–110.
9. Hegi ME, Diserens AC, Gorlia T, et al. MGMT gene silencing and benefit from temozolomide in glioblastoma. *N Engl J Med.* 2005;352(10):997–1003.
10. Sturm D, Witt H, Hovestadt V, et al. Hotspot mutations in H3F3A and IDH1 define distinct epigenetic and biological subgroups of glioblastoma. *Cancer Cell.* 2012;22(4):425–437.
11. Brennan CW, Verhaak RG, McKenna A, et al; TCGA Research Network. The somatic genomic landscape of glioblastoma. *Cell.* 2013;155(2):462–477.
12. Capper D, Jones DTW, Sill M, et al. DNA methylation-based classification of central nervous system tumours. *Nature.* 2018;555(7697):469–474.

13. de Vleeschouwer S, Rapp M, Sorg RV, et al. Dendritic cell vaccination in patients with malignant gliomas: current status and future directions. *Neurosurgery.* 2006;59(5):988–999; discussioin 999.
14. Ardon H, Van Gool S, Lopes IS, et al. Integration of autologous dendritic cell-based immunotherapy in the primary treatment for patients with newly diagnosed glioblastoma multiforme: a pilot study. *J Neurooncol.* 2010;99(2):261–272.
15. Chen YA, Lemire M, Choufani S, et al. Discovery of cross-reactive probes and polymorphic CpGs in the Illumina Infinium HumanMethylation450 microarray. *Epigenetics.* 2013;8(2):203–209.
16. Capper D, Stichel D, Sahm F, et al. Practical implementation of DNA methylation and copy-number-based CNS tumor diagnostics: the Heidelberg experience. *Acta Neuropathol.* 2018;136(2):181–210.
17. Bady P, Delorenzi M, Hegi ME. Sensitivity analysis of the MGMT-STP27 model and impact of genetic and epigenetic context to predict the MGMT methylation status in gliomas and other tumors. *J Mol Diagn.* 2016;18(3):350–361.
18. Garber ST, Hashimoto Y, Weathers SP, et al. Immune checkpoint blockade as a potential therapeutic target: surveying CNS malignancies. *Neuro Oncol.* 2016;18(10):1357–1366.
19. Dejaegher J, Verschuere T, Vercalsteren E, et al. Characterization of PD-1 upregulation on tumor-infiltrating lymphocytes in human and murine gliomas and preclinical therapeutic blockade. *Int J Cancer.* 2017;141(9):1891–1900.
20. Verschuere T, Van Woensel M, Fieuws S, et al. Altered galectin-1 serum levels in patients diagnosed with high-grade glioma. *J Neurooncol.* 2013;115(1):9–17.
21. Berghoff AS, Kiesel B, Widhalm G, et al. Correlation of immune phenotype with IDH mutation in diffuse glioma. *Neuro Oncol.* 2017;19(11):1460–1468.
22. Rutledge WC, Kong J, Gao J, et al. Tumor-infiltrating lymphocytes in glioblastoma are associated with specific genomic alterations and related to transcriptional class. *Clin Cancer Res.* 2013;19(18):4951–4960.
23. Prins RM, Soto H, Konkankit V, et al. Gene expression profile correlates with T-cell infiltration and relative survival in glioblastoma patients vaccinated with dendritic cell immunotherapy. *Clin Cancer Res.* 2011;17(6):1603–1615.
24. Yang I, Tihan T, Han SJ, et al. CD8+ T-cell infiltrate in newly diagnosed glioblastoma is associated with long-term survival. *J Clin Neurosci.* 2010;17(11):1381–1385.
25. Brooks WH, Markesbery WR, Gupta GD, Roszman TL. Relationship of lymphocyte invasion and survival of brain tumor patients. *Ann Neurol.* 1978;4(3):219–224.
26. Palma L, Di Lorenzo N, Guidetti B. Lymphocytic infiltrates in primary glioblastomas and recidivous gliomas. *J Neuroimmunol.* 1978;49(6):854–861.
27. Böker DK, Kalff R, Gullotta F, Weekes-Seifert S, Möhrer U. Mononuclear infiltrates in human intracranial tumors as a prognostic factor. Influence of preoperative steroid treatment. I. Glioblastoma. *Clin Neuropathol.* 1984;3(4):143–147.
28. Kmiecik J, Poli A, Brons NH, et al. Elevated CD3+ and CD8+ tumor-infiltrating immune cells correlate with prolonged survival in glioblastoma patients despite integrated immunosuppressive mechanisms in the tumor microenvironment and at the systemic level. *J Neuroimmunol.* 2013;264(1-2):71–83.
29. Lohr J, Ratliff T, Huppertz A, et al. Effector T-cell infiltration positively impacts survival of glioblastoma patients and is impaired by tumor-derived TGF-β. *Clin Cancer Res.* 2011;17(13):4296–4308.
30. Rossi ML, Jones NR, Candy E, et al. The mononuclear cell infiltrate compared with survival in high-grade astrocytomas. *Acta Neuropathol.* 1989;78(2):189–193.
31. Safdari H, Hochberg FH, Richardson EP Jr. Prognostic value of round cell (lymphocyte) infiltration in malignant gliomas. *Surg Neurol.* 1985;23(3):221–226.
32. Wherry EJ. T cell exhaustion. *Nat Immunol.* 2011;12(6):492–499.
33. Grossman SA, Ye X, Lesser G, et al; NABTT CNS Consortium. Immunosuppression in patients with high-grade gliomas treated with radiation and temozolomide. *Clin Cancer Res.* 2011;17(16):5473–5480.
34. Fadul CE, Fisher JL, Gui J, Hampton TH, Côté AL, Ernstoff MS. Immune modulation effects of concomitant temozolomide and radiation therapy on peripheral blood mononuclear cells in patients with glioblastoma multiforme. *Neuro Oncol.* 2011;13(4):393–400.
35. Kaffes I, Szulzewsky F, Chen Z, et al. Human mesenchymal glioblastomas are characterized by an increased immune cell presence compared to proneural and classical tumors. *Oncoimmunology.* 2019;8(11):e1655360.
36. Schiffer D, Cavicchioli D, Giordana MT, Palmucci L, Piazza A. Analysis of some factors effecting survival in malignant gliomas. *Tumori.* 1979;65(1):119–125.
37. Sayour EJ, McLendon P, McLendon R, et al. Increased proportion of FoxP3+ regulatory T cells in tumor infiltrating lymphocytes is associated with tumor recurrence and reduced survival in patients with glioblastoma. *Cancer Immunol Immunother.* 2015;64(4):419–427.